DOI: https://doi.org/10.4038/sljp.v26i1.8170

INSTITUTE OF PHYSICS – SRI LANKA

Research Article

XRD and optical studies of CdI_2 thin films with varying grain size and thickness for the control of bandgaps

M. Idrish Miah*

Department of Physics, University of Chittagong, Chittagong–4331, Bangladesh.

Abstract

Cadmium iodide (CdI_2) thin films with varying grain size and thickness were studied for exploring the strategy of controlling bandgap (E_g) in the thin film-materials. The grain size (D) was calculated from the X-ray diffraction (XRD) and was found to increase with increasing the thickness (L) of the film. A variation of the refractive index (n) with the variation of L was observed, which might be due to the variation of both density and electronic structure. However, n was found to decrease with increasing the wavelength of light. The optical absorption spectra showed both allowed direct and indirect interband transitions across a fundamental gap. It was found that both indirect and direct E_g decrease with increasing L and that the indirect E_g was lower than the direct E_g, confirming the results of the earlier band structure calculations. The direct E_g was also found to decrease with increasing D. The results demonstrate the possibility of controlling and manipulating E_g by adjusting D and L.

Keywords: Optical properties; Bandgap control; XRD

* Corresponding author: m.idrish.miah@cu.ac.bd

1. INTRODUCTION

Cadmium iodide (CdI_2) is a wide-band gap semiconductor having optical band gap (E_g) near a weak insulator and with highly anisotropic chemical bonds [1] and is an important compound having a layered structure with an infinite hexagonal sheet of Cd atoms sandwiched between two similar sheets of I atoms. The Cd atoms are octahedrally coordinated to constitute the basic layer by a strong covalent bonding within *ab*-plane forming a sheet like structure and these sheets are arranged along the third direction *c* to form a three-dimensional solid. A weak van der Waals bonding between these sheets leads to polytype structures having a number of polytypes [2].

Band structure calculations for CdI_2 have shown [3-5] large anisotropy of the space charge density distribution causing high anisotropy of optical spectra and the presence of a direct E_g and a slightly smaller indirect E_g. CdI_2 is central symmetric or centrosymmetric in the bulk. However, the anisotropic behaviour of CdI_2 makes it polar, so a strong electron-phonon interaction is expected. This favours the local non-centrosymmetricity for the observation of the second harmonic generation (SHG) in CdI_2 nanostructures [6-8]. The role of photo-induced electron-phonon anharmonic interactions in SHG has previously been explored [9].

Stimulated photoluminescence and thermoluminescence studies revealed that this material processes higher order optical nonlinearity [10-14]. Materials exhibiting higher order optical nonlinearities have received much attention due to their potential in applications such as optical switching, amplification and limiting [15]. The ferroelectric was studied by Kityk et al. [16]. This is most probably the first extensive study on CdI_2 thin films.

Having layered structural and nonlinear optical properties make CdI_2 a better candidate for the intensive studies [17]. The various aspects of the layered compounds have thus been investigated for the better understanding and advancing new device ideas. Band gap engineering is a powerful technique for the design of new semiconductor materials and devices [18,19]. In this process, the transport properties of electrons and holes could be independently and continuously tuned for a given application or device (e.g. photomultiplier). The experimental demonstration on the band gap engineering of layered hexagonal $SnSe_2$ nanostructured thin films by varying the thickness was first given by Mukhokosi et al. [20]. They showed that for a 50-nm thick film, the band gap E_g is about 2.04 eV, whereas E_g is

approximately 1.2 eV for the bulk or 1200-nm thick film. Their study highlights the possibility of engineering the band gap of layered CdI_2 by controlling the thickness of the films. In a recent study, CdI_2 thin films were grown by chemical bath deposition and their crystalline structure and linear optical properties including optical band gap were controlled by changing the pH of the chemical bath at room temperature [21]. Dependence of E_g on residual stress in ZnI_2, CdI_2 and HgI_2 films was also studied [22]. However, studies focusing on the optical bandgap and its related properties are quite limited for CdI_2 thin films. As the new generation of devices with unique capabilities is emerging from this approach, it would be worthy to carry out a systematic and intensive study on this issue in CdI_2 thin films. In the present investigation, we study the optical properties and the dependence of the direct and indirect bandgaps on the grain size and film thickness of CdI_2 thin film.

2. EXPERIMENTAL

Thin films of CdI_2 were grown on glass substrates at room temperature by evaporation using a molybdenum boat. The typical glass substrates were 2.5 cm × 5 cm sizes. The starting material was high purity (99.99%) analar grade powder that was palletized for evaporation. All the CdI_2 films used in this study were grown at the vacuum of 10^{-6} Torr. The film thickness was monitored by a quartz crystal thickness monitor during evaporation and subsequently confirmed by DEKTAK IIA surface profiler measurements. The structural study was carried out by X-ray-diffraction (XRD) analysis (PHILIPS, Model PW-1830). The film composition of the as grown films was found to be stoichiometric. However, no significant deviation from stoichiometric film composition was observed for heat-treated films or films grown at substrate temperatures up to a couple hundred $^{\circ}$C. The optical absorption measurements were carried out in the UV-Visible region using a Shimadzu UV-260 spectrophotometer.

3. RESULTS AND DISCUSSION

We carried out XRD measurements on a large number of thin film samples. XRD based structural, compositional and morphological studies on this material are available in the literature [19,20]. For this reason, XRD spectra and their same details are not given here. The grain size (D) of the material was calculated using the well-known Debye-Scherrer formula [23] $D = 0.9\lambda / (H\cos\theta)$, where H is the half width of XRD lines, λ is its wavelength and θ is

the half diffraction angle (i.e. Bragg angle) of 2θ. Film thickness was obtained from the relation $L = D^3 N$, where N is the number of crystallites per unit area. Grain size D as a function of film thickness (L) is shown in Fig. 1. As the figure depicts, D increases with increasing film thickness. As can be seen the grain size varies from 110 nm to 160 nm for the film thickness 50 nm to 550 nm. The dislocation density (S) can also be obtained from the relation $S = 1/D^2$.

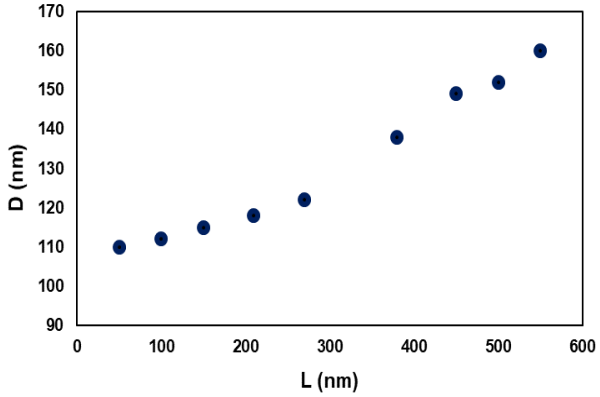

Figure 1. Grain size as a function of film thickness measured from X-ray diffraction.

We performed optical absorption and reflectance measurements on a large number of samples with different thicknesses. The reflectance (r) was measured at various wavelengths λ and film thicknesses. The r was found to decrease with increasing λ. The refractive index (n) was calculated from the data of reflectance using the relation

$$n = \frac{1+r}{1-r} + \sqrt{\frac{4r}{(1-r)^2} - \left(\frac{\alpha\lambda}{4\pi}\right)^2}, \tag{1}$$

where α is the absorption coefficient and is related to the extinction coefficient (β) as $\beta = \alpha\lambda/(4\pi)$. The refractive index as a function of L is shown in Fig. 2, where n decreases with λ. The dependence of n on L shows an oscillating behavior. This variation of n with L might be due to the variations of both density and electronic structure. The density effect can be estimated as (n^2 – 1) is inversely proportional to the unit cell volume. For our system of hexagonal unit cell the volume is $0.866a^2c$. Because of the thickness independent lattice

constant a, $(n^2 - 1)$ is proportional to $1/c$. This demonstrates the dominance of density effect in the thickness dependence of n.

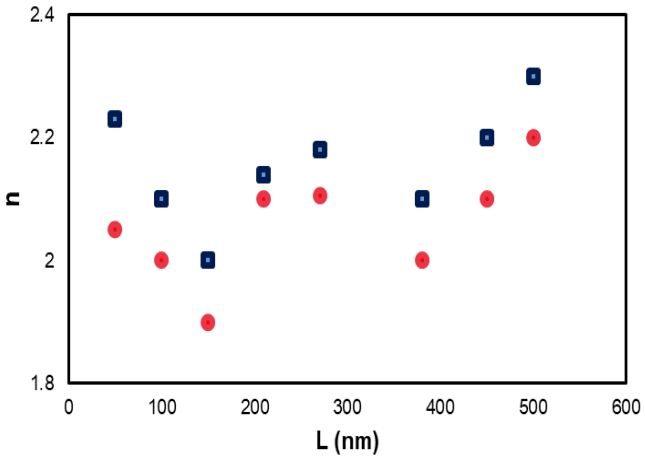

Figure 2: Refractive index n as a function of L for wavelengths λ = 600 nm (square) and 760 nm (circle).

For the direct type of transition, the conduction band (CB) minimum and the valance band (VB) maximum is in line on the energy (E) scale in the E-k diagram, where $k = 2\pi / \lambda$ is the wave vector (Fig. 3). However, it deviates for the phonon-assisted indirect transition, as there are phonons involved in the process. Therefore, the band gap E_g is the energy difference between the CB minimum and VB maximum, or the energy difference between the CB and VB at $k = 0$.

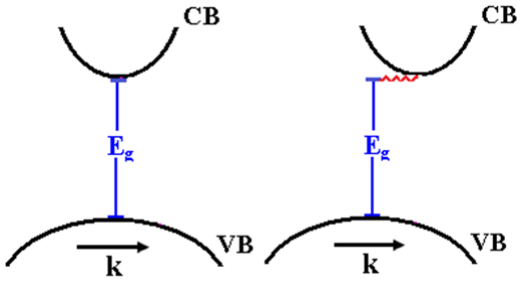

Figure 3. Direct (left) and phonon-assisted or indirect (right) band gap E_g as a function of the wave vector k. E_g is the energy difference between the conduction band (CB) minimum and the valance band (VB) maximum, or the energy difference between the CB and VB at $k = 0$. In indirect E_g, the phonon involvement is indicated by a wave.

The absorption coefficient α was calculated from the data of optical absorption measurements using the relation $\alpha = 2.303A/L$, where A is the absorbance, neglecting the reflection which is insignificant near the absorption edge. The optical absorption shows both allowed direct and indirect interband transitions across a fundamental gap confirming the results of the earlier band structure calculations for the optical direct and indirect band gap E_g in CdI_2 thin films. Figure 4 shows a typical absorption spectrum of the material, where the dependence of α on E_λ is plotted near the absorption edge. Here $E_\lambda = h\nu = hc/\lambda$ is the of excited photon energy.

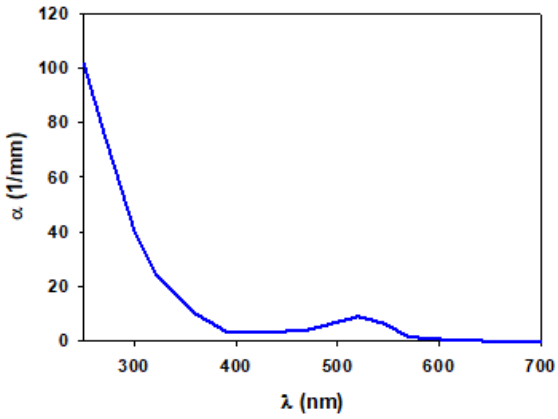

Figure 4: A typical absorption spectrum. The absorption coefficient α was calculated from the absorbance and the film thickness.

In crystalline materials and for parabolic bands, as shown in Fig. 3, the optical transitions (either direct or indirect) can be evaluated by the relation between α and E_g. For the direct transition

$$\alpha E_\lambda = C_1(E_\lambda - E_g)^p \tag{2}$$

and for the indirect transition

$$\alpha E_\lambda = \frac{C_2(E_\lambda - E_g + E_{ph})^p}{\exp(\Theta_D/T) - 1} + \frac{C_3(E_\lambda - E_g - E_{ph})^p}{1 - \exp(-\Theta_D/T)} \tag{3}$$

where C_1, C_2 and C_3 are fitting constants, Θ_D is the Debye temperature, E_{ph} is the phonon energy assisting the indirect transition, and for a direct (indirect) type of transition p = 1/2 or 3/2 (p = 2 or 3) depending on whether the transition is allowed or forbidden [24,25]. The optical band gap E_g of CdI_2 thin films was estimated from Tauc plot. The Tauc technique of determining E_g is to plot a $(\alpha E_\lambda)^{1/p}$ versus E_λ graph and look for that value of p which gives

the best linear fit in the absorption. For an allowed transition p = 1/2 (p = 2) for a direct (indirect) type. As can be seen, there will be one (two) linear region(s) for the direct (indirect) transition. We plotted $(\alpha E_\lambda)^{1/p}$ versus E_λ for the films of various thicknesses and discovered both type of allowed transitions. Figures 5 and 6 show the results. A linear fit to the data of the higher wavelength region of the graph gives a direct E_g as an intercept of the vertical axis (Fig. 5). Similarly, two lines fitted to the data of the low and high wavelength regions of the graph give the indirect type E_g (Fig. 6).

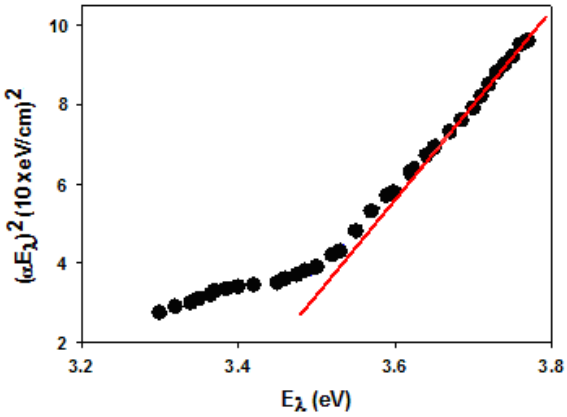

Figure 5: Plot of $(\alpha E_\lambda)^2$ versus E_λ with $E_\lambda = h\nu = hc/\lambda$. Red line is a linear fit to the data of the higher wavelength region of the absorbed photon energy curve.

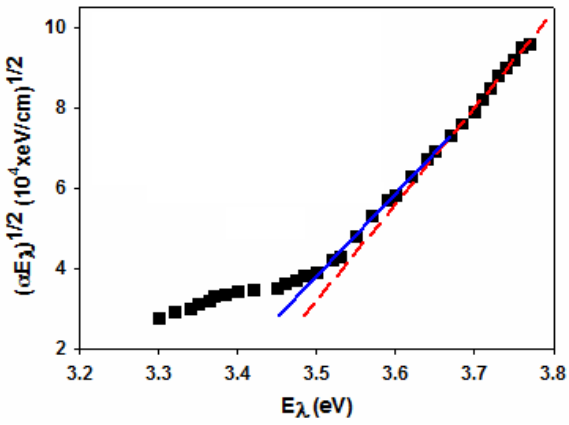

Figure 6: Plot of $(\alpha E_\lambda)^{1/2}$ versus E_λ. Lines are linear fits to the data of the low (blue solid) and high (red dashed) wavelength regions of the curve.

Figure 7 shows the dependence of E_g on L for the direct and indirect transitions. As can be seen, the optical band gap E_g for both direct and indirect types varies with the thickness of the

film. This variation looks like quadratic in nature. The direct (indirect) E_g is found to vary from about 3.05 to 3.65 eV (2.50 to 3.20 eV) for the variation of film thickness from 400 nm to 5.5 μm. This variation consists well with that for the other layered hexagonal $SnSe_2$ nanostructured thin films [20].

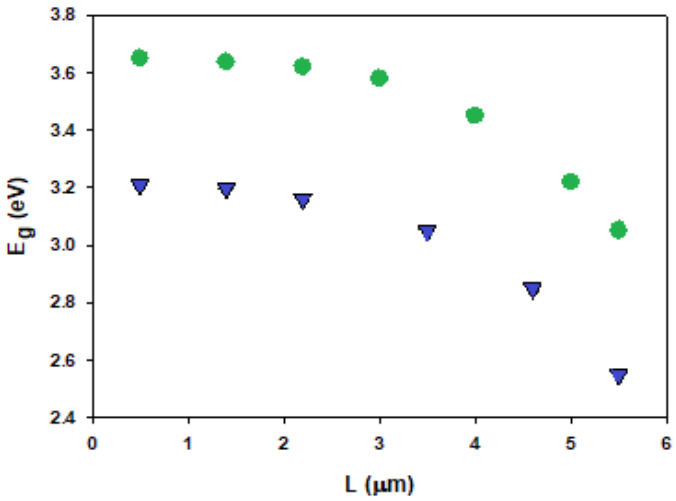

Figure 7: E_g as a function of L for the direct and indirect transitions between parabolic bands. Here, closed circles are for direct and closed triangles are for indirect transitions.

The increase of E_g with L may be attributed to the formation of crystal defects, which can produce localized states that change the effective Fermi level due to an increase in carrier concentrations [14]. Tyagi et al. [22] studied the variation of E_g of CdI_2 thin films, grown on glass substrate, with residual stress parameter and showed that there exists a threshold tensile stress above which E_g decreases linearly. They found a direct E_g of 3.60 eV for the film. The possible optical transition in these films was found to be allowed direct transition with the E_g decreasing from 3.76 to 3.57 eV with increasing the film thickness [26]. Our values agree well with these. A slight decease of our values might be responsible for the growth conditions which affect the formation of the defects. This could reduce the concentration of localized states in band structure. However, the band gap E_g for the indirect transition is lower than that of the direct transition by an amount of ~0.7 eV, which is due to the phonon assisted transition. The dependence of E_g on D for the direct transition is shown in Fig. 8. For the higher D, the dependence is seen to be linearly decreasing with increasing D.

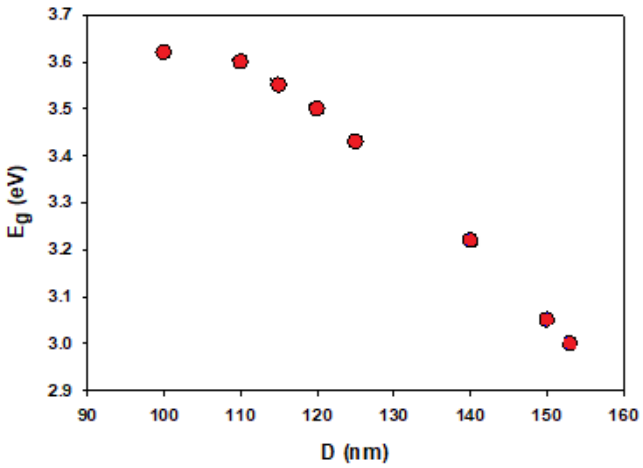

Figure 8: E_g as a function of D for the direct transition. For higher values of D, the dependence is linear.

4. CONCLUSIONS

We grew CdI_2 thin films with various grain sizes and thicknesses by thermal evaporation and studied Optical bandgap E_g by XRD. The grain size was found to increase with increasing the thickness of the film. A variation of the refractive index with the variation of the film thickness was observed, which might be due to the variations of both density and electronic structure. The refractive index was found to decrease with increasing the wavelength of light. The optical absorption spectra showed both allowed direct and indirect interband transitions across a fundamental gap. It was found that both indirect and direct E_g decrease with increasing thickness of the film and that the indirect E_g was lower than the direct E_g. The results were discussed in comparison with those in the literature.

Conflicts of interest

The author declares no conflicts of interest.

References

[1] N. F. Mott, E. A. Davis, Electronic Processes in Non-crystalline Materials (Clarendon Press, Oxford, 1979).

[2] F. Hulliger, In: Levy F, Reidel D, eds. Structural chemistry of layer-type phases. Holland: Dordrecht-Holland; 1976. p. 31–4.

[3] J. Bordas, J. Robertson, A. Jakobsson, J. Phys. C 11 (1978) 2607.

[4] J. Robertson, J. Phys. C 12 (1979) 4753.

[5] M. R. Tubbs, J. Phys. Chem. Solids 26 (1968) 1191.

[6] M. I. Miah, J. Appl. Phys. 104, 064313 (2008).

[7] M. I. Miah, J. Phys. Chem. B 113, 1652 (2009).

[8] H. Ollafsson, and F. Stenberg, Opt. Mater. 341 (2004).

[9] M. I. Miah and J. Kasperczyk, Appl. Phys. Lett. 94, 053117 (2009).

[10] Z. Spurny, Nucl. Instr. Methods 175, 71 (1980).

[11] I. M. Catalano, A. Cingolani, R. Ferrara, and M. Lepore, Helv. Phys. Acta 58 (1985) 329.

[12] F. Adduci, A. Cingolani, R. Ferrara, M. Lugara, and A. Minafra, Nuova Cimento B 38, 610 (1977).

[13] M. I. Miah, Opt. Mater. 18, 231 (2001).

[14] M. I. Miah, Phys. Lett. A 374, 75 (2009).

[15] M. I. Miah, Optik- Intern. J. Light Electron Opt. 123, 1580 (2012).

[16] I. V. Kityk, S. A. Pyroha, T. Mydlarz, J. Kasperczyk, and M. Czerwinski, Ferroelectrics 205, 107 (1998).

[17] M. I. Miah, Eur. Phys. J. B 92, 224 (2019).

[18] F. Capasso, Science 235, 172 (1987).

[19] A. Sitt, I. Hadar, U. Banin, Nanotoday 8, 494 (2013).

[20] E. P. Mukhokosi, S. B. Krupanidhi, and K. K. Nanda, Sci. Rep. 7, 15215 (2017).

[21] I. A. Kariper, J. Mater. Res. Technol. 5, 77 (2016).

[22] P. Tyagi , R. K. Mishra , N. C. Mehra, and A. G. Vedeshwar, Integ. Ferroelectr. 122, 52 (2010).

[23] R. S. Rawat, P. Arun, A. G. Vedeshwar, P. Lee, S. Lee, J. Appl. Phys. 95, 7725 (2004).

[24] J. J. Pankove, Optical processes in semiconductors and conductors, Prentice Hall, Englewood Cliffs, New York, 1971.

[25] J. C. Slater, Phys Rev 103, 1631 (1956).

[26] I. S. Yahia, M. Shapaan, Y. A. M. Ismail, A. M. Aboraia, E. R. Shaaban, J. Alloys Comp. 636 (2015) 317–322.